Protection of states and braiding-based operations in the Majorana qubit

(Dated: March 20, 2018)

Last week, we have discussed simple quantum information protocols using a Kitaev double dot, a minimal model for 1D topological superconductors. In this lecture, we extend the discussion to larger system sizes and the presence of disorder. We discuss that quantum information encoded in a multi-site disordered Majorana qubit is protected against certain types of environmental disturbances. We also argue that a special type of operation, called 'braiding', provides a means to perform certain quantum-logical gates on a Majorana qubit in a way that is protected against errors. This implies that experiments with Majorana qubits could play a pivotal role in exploring fundamental aspects of quantum dynamics; however, the robust operations in this setup are insufficient for universal quantum computing.

CONTENTS

CONTRIBUTORS

Andras Palyi (writeup), Janos Asboth, Peter Boross, Laszlo Oroszlany, Gabor Szechenyi, Janos Asboth (discussions).

I. A LONG, DISORDERED TOPOLOGICAL KITAEV CHAIN HAS A TWOFOLD DEGENERATE GROUND STATE

1. Consider a Kitaev chain with N_{site} sites. Using the notation of the last lecture, the topological fully dimerized Kitaev chain is defined as $\epsilon = 0$, $\Delta = v$. Here we show that such an (ordered) Kitaev chain has a twofold degenerate ground state. (Actually, this implies that all energy eigenstates are twofold degenerate.) Furthermore, the two ground states have different fermion-number parity (even, odd).

2. Consider the example of the 3-site Kitaev wire in the topological fully dimerized limit.

$$H = v(c_1^\dagger c_2 + c_2^\dagger c_3 + h.c.) + v(c_1^\dagger c_2^\dagger + c_2^\dagger c_3^\dagger + h.c.). \tag{1}$$

We are interested in the excitation spectrum of an N_{site}-long chain, but start out with this simple illustrative example. The BdG matrix reads

$$\mathcal{H} = v \begin{pmatrix} 0 & 1 & 0 & 0 & 1 & 0 \\ 1 & 0 & 1 & -1 & 0 & 1 \\ 0 & 1 & 0 & 0 & -1 & 0 \\ 0 & -1 & 0 & 0 & -1 & 0 \\ 1 & 0 & -1 & -1 & 0 & -1 \\ 0 & 1 & 0 & 0 & -1 & 0 \end{pmatrix} \tag{2}$$

Just by inspection, it is clear that there are two zero BdG eigenvalues, and the corresponding BdG eigenvectors are $\psi_{1+} = (1,0,0,1,0,0)/\sqrt{2}$ and $\psi_{3-} = (0,0,1,0,0,-1)/\sqrt{2}$. We call them them zero modes. It is straightforward to see that two zero-eigenvalue eigenvectors with the same edge-localized structure exist for an arbitrary

chain length $N_{\rm site} \geq 2$. Other, similarly defined BdG vectors $\psi_{m\pm}$ do not seem to be zero modes. We know that the 'positive part' of the BdG spectrum corresponds to the quasiparticle excitation energies. Having a twofold degenerate zero eigenvalue, and assigning one of them a 'positive' label, we conjecture that the ground state of a topological fully dimerized Kitaev chain of any length is twofold degenerate.

3. *The edge-localized zero modes are not fermionic.* The generic feature of the BdG approach is that we associate to the eigenvectors φ_α of the BdG matrix ($\alpha = 1, 2, \ldots, 2N_{\rm site}$) quasiparticle annihilation operators $d_\alpha = \boldsymbol{\varphi}_\alpha^\dagger \tilde{\boldsymbol{c}}$, that have fermionic character, e.g., $\{d_\alpha, d_\alpha\} = 0$. It is easy to show that the BdG vector φ_α provides a fermionic operator only if it is orthogonal to its particle-hole partner, $\langle \sigma_x K \varphi_\alpha | \varphi_\alpha \rangle = 0$. This is automatically fulfilled for non-zero modes. However, the zero modes above are not fermionic, as they are proportional to their own particle-hole partners.

4. *The edge-localized zero modes can be chosen to be Majorana-type.* Majorana-type zero modes are defined as being equal to their particle-hole partner: $\sigma_x K \chi = \chi$. In the example of the 3-site Kitaev chain above, $\chi_{1+} = \psi_{1+}$ and $\chi_{3-} = -i\psi_{3-}$ are of Majorana type. The corresponding quasiparticle operators, e.g., $a_{1+} = \boldsymbol{\chi}_{1+}^\dagger \tilde{\boldsymbol{c}}$, are self-adjoint, and obey non-fermionic anticommutation relations: Although they fulfill the fermionic relation $\{a_{1+}, a_{1+}^\dagger\} = 1$, but they show the non-fermionic relation $\{a_{1+}, a_{1+}\} = 1$; the fermionic version would have zero on the right hand side. Note that the latter relation implies $a_{1+}^2 = 1/2$. Note also that two orthogonal Majorana zero modes χ_1 and χ_2 can be superposed, e.g., as $\varphi = (\chi_1 + i\chi_2)/\sqrt{2}$, to form a fermionic zero mode:

$$\langle \sigma_X K \varphi | \varphi \rangle = \langle \chi_1 - i\chi_2 | \chi_1 + i\chi_2 \rangle / 2 = 1/2 - 1/2 = 0. \tag{3}$$

5. *The topological fully dimerized Kitaev chain has a twofold degenerate ground state.* Having two Majorana zero modes in the 3-site Kitaev chain example implies that we have a single zero-energy fermionic excitation, that is, the ground state is twofold degenerate, one has even, the other has odd fermion partity; in analogy with the Kitaev double dot. This implies that all quantum information schemes discussed for the Kitaev double dot generalize for longer topological fully dimerized Kitaev chains as well.

6. *Protection of zero modes against disorder.* A natural question: is the ground state of a finite topological Kitaev chain degenerate, even outside of the fully dimerized limit? Is this degeneracy robust against disorder? At least to an exponentially good approximation, similarly to the zero-energy degeneracy of the SSH model? The answer is: yes. The argument is the same as in the SSH model: (i) A topological fully dimerized half-infinite Kitaev chain has a zero mode at its edge. (ii) Deviations from the fully dimerized case and moderate quadratic disorder can extend the localization length ξ of the zero mode. However, it cannot remove its BdG eigenvalue from zero, because any quadratic disorder Hamiltonian respects the particle-hole symmetry, and therefore the self-dual character of the zero mode is unchanged by disorder, and therefore its BdG eigenvalue sticks to zero. (iii) For an open finite chain that is much longer than the localization length, $\xi \ll N_{\rm site}$, a minigap can be opened due to the hybridization of the two edge-localized zero modes, but that minigap is exponentially suppressed, $E_{\rm gap} \propto e^{-N_{\rm site}/\xi}$, as long as there are no long-range terms in the Hamiltonian that could directly connect the two zero modes. Note that the chiral symmetry protecting the zero modes in the SSH model is broken by many types of disorder (e.g., on-site disorder) but the protection in the Kitaev chain based on particle-hole symmetry is much stronger: any quadratic perturbation, including on-site energy variations or pair-potential variation, respects particle-hole symmetry.

II. THE FERMION-PARITY PSEUDOQUBIT IS PROTECTED AGAINST DISORDER-INDUCED DEPHASING

1. Adjectives to be added in front of 'disorder': moderate; slow; local; quadratic.

2. Trivial: FPPQ is protected against relaxation.

3. Protection from disorder-induced dephasing is suggested by the fact that the minigap is $E_{\rm gap} \propto e^{-N_{\rm site}/\xi}$, so the Hamiltonian of the low-energy FPPQ subspace spanned by $|e\rangle$ and $|o\rangle$ is essentially zero.

4. Nevertheless, an additional argument is provided here:

$$\begin{aligned}\langle o|H_p|o\rangle - \langle e|H_p|e\rangle = \langle \varphi_1|\mathcal{H}_p|\varphi_1\rangle &= \frac{1}{\sqrt{2}}\left(\langle\chi_L| - i\langle\chi_R|\right)\mathcal{H}_p\frac{1}{\sqrt{2}}\left(|\chi_L\rangle + i|\chi_R\rangle\right) \\ &= \frac{1}{2}\left(\langle\chi_L|\mathcal{H}_p|\chi_L\rangle + \langle\chi_R|\mathcal{H}_p|\chi_R\rangle + \langle\chi_L|\mathcal{H}_p|\chi_R\rangle + \langle\chi_R|\mathcal{H}_p|\chi_L\rangle\right) \sim e^{-N_{\rm site}/\xi}.\end{aligned} \tag{4}$$

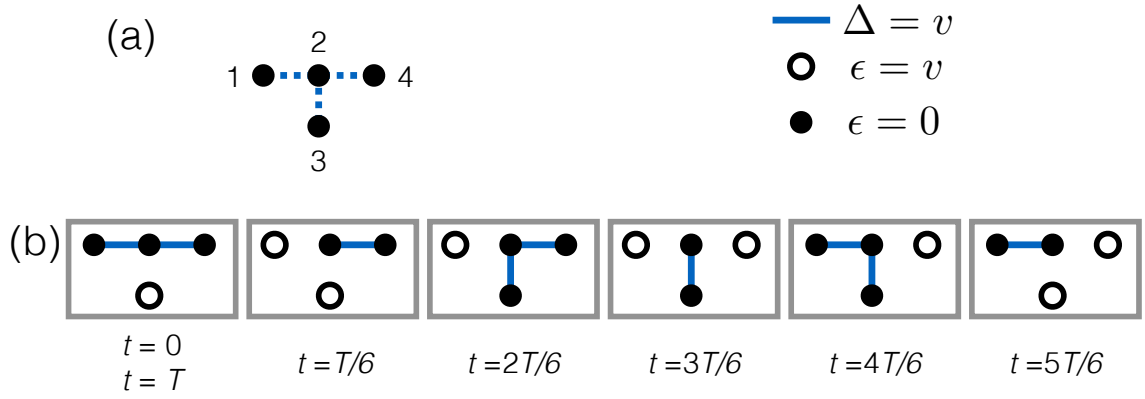

FIG. 1. **An example braiding protocol in a 4-site Kitaev setup.**

Here, φ_1 is the fermionic zero mode corresponding to the $|e\rangle \mapsto |o\rangle$ excitation. In this result, the last two term are exponentially small, as they arise from the overlap of the two different zero modes. Furthermore, the first two term vanish due to the built-in particle-hole symmetric nature of the perturbation BdG matrix and the Majorana character of the zero modes:

$$\langle\chi|\mathcal{H}_1|\chi\rangle = -\langle\chi|\sigma_x K\mathcal{H}_1\sigma_x K|\chi\rangle = -\langle\sigma_x K\chi|\mathcal{H}_1\sigma_x K|\chi\rangle^* = -\langle\chi|\mathcal{H}_1|\chi\rangle^* . \tag{5}$$

Note also that the first equality in Eq. (4) is rigorous,

$$\langle o|H_p|o\rangle - \langle e|H_p|e\rangle = \langle e|d_1 H_p d_1^\dagger|e\rangle - \langle e|H_p|e\rangle = \langle e|\frac{1}{2}d_1\tilde{\boldsymbol{d}}^\dagger\mathcal{H}_p\tilde{\boldsymbol{d}}d_1^\dagger|e\rangle - \langle e|\frac{1}{2}\tilde{\boldsymbol{d}}^\dagger\mathcal{H}_p\tilde{\boldsymbol{d}}|e\rangle \tag{6}$$

$$= \langle e|\frac{1}{2}d_1 d_1^\dagger\mathcal{H}_{p,11}d_1 d_1^\dagger|e\rangle + \sum_{n=2}^{N_{\rm site}}\langle e|\frac{1}{2}d_1 d_n\mathcal{H}_{p,N_{\rm site}+n,N_{\rm site}+n}d_n^\dagger d_1^\dagger|e\rangle \tag{7}$$

$$-\sum_{n=1}^{N_{\rm site}}\langle e|\frac{1}{2}d_n\mathcal{H}_{p,N_{\rm site}+n,N_{\rm site}+n}d_n^\dagger|e\rangle = \mathcal{H}_{p,11} \equiv \langle\varphi_1|\mathcal{H}_p|\varphi_1\rangle . \tag{8}$$

5. *Readout of the FPPQ using local observables is exponentially difficult.* This is a consequence of Eq. (4), which implies that the expectation value of any local observable (e.g., charge density at site 3) is very much the same in the two ground states. This is a rather surprising fact, since the two ground state are obviously very different, e.g., they are orthogonal to each other. To be able to distinguish between the two ground states using local observables, one has to make the overlap of the zero modes significant (e.g., the reduce the chain length, or increase the penetration length).

III. BRAIDING PROVIDES AN S GATE FOR THE FERMION-PARITY PSEUDOQUBIT

1. For a generic qubit, the S gate is defined as

$$S = \begin{pmatrix} e^{i\pi/4} & 0 \\ 0 & e^{-i\pi/4} \end{pmatrix} = \begin{pmatrix} \frac{1+i}{\sqrt{2}} & 0 \\ 0 & \frac{1-i}{\sqrt{2}} \end{pmatrix} = e^{-i\frac{\pi}{4}\sigma_z} \equiv \begin{pmatrix} 1 & 0 \\ 0 & i \end{pmatrix} = \begin{pmatrix} 1 & 0 \\ 0 & e^{i\pi/2} \end{pmatrix} . \tag{9}$$

The claim is that during braiding, that is, exchanging the two ends of a Kitaev chain forming an FPPQ, $|e\rangle$ evolves into some $|e(T)\rangle = e^{i\varphi}|e\rangle$ and $|o\rangle$ evolves into $|o(T)\rangle = e^{i(\varphi+\pi/2)}|o\rangle$; hence braiding realizes an S gate on the FPPQ.

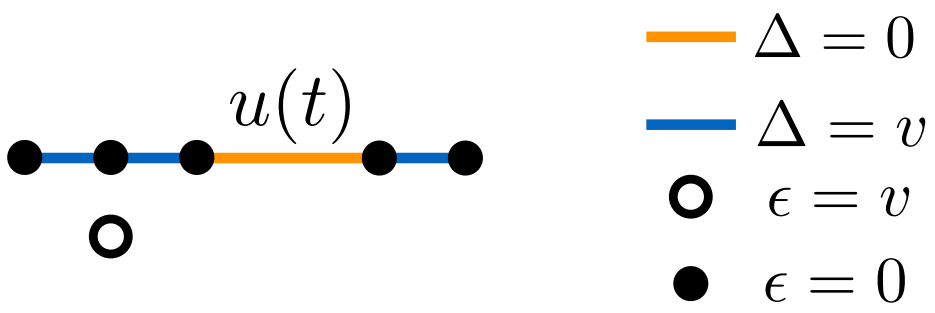

FIG. 2. **A simple setup to test that braiding works.**

2. A simple example of braiding, using a 4-site setup, is shown in Fig. 1. The Hamiltonian reads

$$H = \sum_{m=1}^{4} \epsilon_m(t) c_m^\dagger c_m + v_{12}(t)\left(c_1^\dagger c_2 + c_1^\dagger c_2^\dagger + h.c\right) + v_{23}(t)\left(c_2^\dagger c_3 + c_2^\dagger c_3^\dagger + h.c\right) + v_{24}(t)\left(c_2^\dagger c_4 + i c_2^\dagger c_4^\dagger + h.c\right) \quad (10)$$

where the site numbering is defined in Fig. 1a. As indicated in the legend of Fig. 1a, parameters are tuned in time, continuously between 0 and v, to complete the 7-stage cycle shown in Fig. 1b. The deformation of the Hamiltonian is assumed to be slow, adiabatic, $T \gg \hbar/v$. It is an instructive exercise to numerically calculate the time evolution of the two initial states $|e\rangle$ and $|o\rangle$, and calculate the T-dependence of the relative phase $\alpha_{\rm rel}(T)$ via

$$e^{i\alpha_{\rm rel}} = \frac{\langle o|o(T)\rangle}{\langle e|e(T)\rangle}. \quad (11)$$

It is expected that the function $\alpha_{\rm rel}(T)$ will show a plateau at $\pi/2$ for slow braiding $T \gg \hbar/v$.

3. This 'braiding' is a cyclic deformation of the Hamiltonian, during which the two ends of the 3-site Kitaev chain are exchanged. Such a protocol is often said to perform the 'braiding of two Majorana zero modes'.

4. Exercise: Fig. 1a shows an anticlockwise braiding. Demonstrate, e.g., numerically, that a clockwise braiding realizes $S^\dagger$.

5. *Simple experiment to test that braiding works.* Of course, the effect of braiding is not observable, as long as we have an FPPQ only. A simple experiment demonstrating braiding could be based on a Majorana qubit with 6 sites is shown in Fig. 2. A hopping pulse $u(t)$ (no pair potential involved), similar to those discussed in lecture 4, can be used to perform a $\pi_x/2$ pulse on the Majorana qubit, and thereby prepare a superposition, $|ee\rangle \mapsto \frac{1}{\sqrt{2}}(|ee\rangle + i\,|oo\rangle)$. Then, braiding, i.e., exchange of the two ends of the left Kitaev chain on the left 4-site unit results in the state $|ee\rangle \mapsto \frac{1}{\sqrt{2}}(|ee\rangle - |oo\rangle)$. (i) A parity readout yields $P_e = 1/2$. (ii) A parity readout following a second $\pi_x/2$ pulse yields $P_e = 1/2$, showing that we had an x-aligned qubit after braiding. (iii) One could suspect that the 1/2 outcomes of (i) and (ii) are due to complete loss of information of the qubit. To show that it's not the case, one could do two braidings, and apply the second $\pi_x/2$ pulse afterwards; this should yield $P_e = 1$ in the absence of decoherence. Of course, all this could be refined, e.g., by doing a more sophisticated, tomography-type experiment.

IV. BRAIDINGS ARE NON-ABELIAN AND PROVIDE TWO-AXIS ROTATIONS FOR THE MAJORANA QUBIT

1. *Braidings in a Majorana qubit.* Consider the Majorana qubit in Fig. 3. The basis states are $|ee\rangle$ and $|oo\rangle$. It is straightforward to see that the braiding of 1 and 2, say, by utilizing the leftmost four sites in Fig. 3a, results in an S gate, $B_{12} = S$. Analogously, $B_{34} = S$. We claim that the braiding of 2 and 3, which is depicted in the sequence of subfigures Fig. 3a-e, results in

$$B_{23} = \frac{1}{\sqrt{2}}\begin{pmatrix} 1 & -i \\ -i & 1 \end{pmatrix} = e^{-i\frac{\pi}{4}\sigma_x}. \quad (12)$$

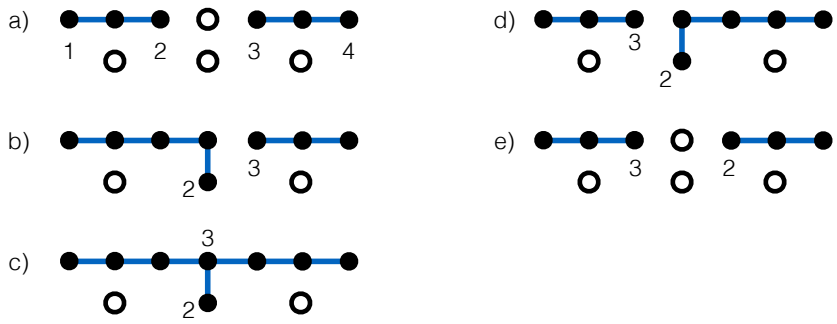

FIG. 3. **Braiding of two Majorana zero modes (2 and 3) on different Kitaev chains.**

We omit the proof here. Of course, this could still be checked using numerical simulation of the dynamics. We encourage the reader to try to do an theory (i.e., non-numerical) proof using the concepts and methods introduced in the next section.

2. *Braidings are non-abelian.* That is, the effect of two braidings depends on the order that they are performed:

$$[B_{12}, B_{23}] = -i\sigma_y \neq 0. \tag{13}$$

3. *Braiding-based quantum gates are non-universal for quantum computing.* These two gates are insufficient for universal quantum computing. One universal gate set is Hadamard, S, $T = e^{-i\sigma_z \pi/8}$, and CNOT. Not sure how to perform Hadamard and CNOT with braiding. Should depend on the encoding (sparse or dense) as well. T is certainly not realized by braiding.

V. BRAIDING-BASED QUANTUM GATES ARE PROTECTED AGAINST DISORDER

1. We have discussed braiding-based quantum gates as well as non-braiding-based quantum gates. Why bother with braiding-based ones, when they look more complicated? Because they are believed to be more robust, i.e., less prone to errors in the presence of disorder.

2. Take a long chain, including disorder, and a braiding protocol $h : [0, 1] \to \text{Hamiltonians}, p \mapsto h(p)$. The braiding dynamics depends on the speed of the variation of the Hamiltonian, that is, on the braiding time T, and is governed by the Hamiltonian $H(t) = h(t/T)$. At each point during the protocol, there is an instantaneous minigap $2E_1(p)$ due to the finite size and the disorder; here E_1 is the lowest positive eigenvalue of the BdG matrix. We use E_{gap} to denote the maximum of this minigap over the cycle, $E_{\text{gap}} = \max_{p\in[0,1]} 2E_1(p)$. When we say that 'braiding provides a robust quantum gate', then we mean that a target gate fidelity arbitrarily close to 1 can be reached by using a large enough system size and a long enough braiding time. In practice, that probably means that as long as there is a large mismatch between the minigap E_{gap} (smaller) and the bulk quasiparticle gap E_{bulk} (greater), then a decent-quality gate can be performed for intermediate times $\hbar/E_{\text{bulk}} \ll T \ll \hbar/E_{\text{gap}}$, and by making the chain larger, and thereby suppressing the minigap, the quality of the gate can be improved, most probably using a longer braiding time T.

3. Note that effects of noise (uncontrolled interactions with the environment, described either as classical or quantum noise) are excluded at this point. Including them could make a qualitative change: The above statement suggests that without noise, the optimal-fidelity braiding duration T would grow with increasing system size, but that would actually give noise more time to influence the dynamics, and thereby potentially reduce the gate fidelity.

4. In the rest of this section, we show that braiding of Majorana zero modes, e.g., exchanging the two ends of a Kitaev chain, results in an S gate on the corresponding FPPQ. The two cornerstones of the proof: (i) particle-hole symmetry of the BdG matrix, (ii) although the relevant quantities are defined via the complete many-body wave function, they can also be expressed in terms of the adiabatic dynamics of the BdG wave functions governed by the (single-particle) time-dependent BdG equation.

5. Step 1: For the proof, we need to show that for the relative phase factor that

$$e^{i\alpha_{\rm rel}} = \frac{\langle o|o(T)\rangle}{\langle e|e(T)\rangle} = e^{i\pi/2} = i. \tag{14}$$

6. Step 2: Clearly, it is rather hopeless to solve the time-dependent Schrödinger equation and use its many-body solution to provide a proof for (14). So we follow a different strategy. Recall that the Fock-space propagator is

$$U(t) = Te^{-\frac{i}{\hbar}\int_0^t dt' H(t')}, \tag{15}$$

and the Heisenberg representation of an arbitrary operator A is $A_H(t) = U^\dagger(t)AU(t)$. Using these, the overlap above is expressed as

$$\langle o|o(T)\rangle = \langle o|U(T)|o\rangle = \langle e|d_1U(T)d_1^\dagger|e\rangle = \langle e|U(T)U^\dagger(T)d_1U(T)d_1^\dagger|e\rangle = \langle e|U(T)d_{1H}(T)d_1^\dagger|e(T)\rangle\,, \tag{16}$$

where $d_1 = \frac{1}{\sqrt{2}}(a_L + ia_R)$ is the fermionic zero mode ($E_1 = 0$) of the initial Hamiltonian $H(0) = h(0)$, and a_L and a_R are the Majorana zero modes localized at the left/right edges. The corresponding BdG vectors are φ_1, χ_L and χ_R, and their relation is $\varphi_1 = \frac{1}{\sqrt{2}}(\chi_L + i\chi_R)$. Here and henceforth, we will neglect the overlap of the Majorana zero modes.

7. Step 3: It seems that the Heisenberg time evolution of the initial quasiparticles will be useful in evaluting the relative phase. It is rather straightforward to show that Heisenberg representation of the initial quasiparticles is known as soon as we know the solutions of the time-dependent BdG equation (that is, the 'BdG propagator'):

$$\tilde{\boldsymbol{d}}_H(t) = \mathcal{U}(t)\tilde{\boldsymbol{d}},\ \text{that is, } \tilde{d}_{\alpha H}(t) = \sum_{\beta=1}^{2N_{\rm site}} \mathcal{U}_{\alpha\beta}(t)\tilde{d}_\beta,\ \text{where } (\alpha = 1, 2, \ldots, 2N_{\rm site}), \tag{17}$$

where the BdG propagator is

$$\mathcal{U}(t) = Te^{-\frac{i}{\hbar}\int_0^t dt'\mathcal{H}(t')},\ \text{and } \mathcal{U}_{\alpha\beta}(t) = \langle\varphi_\alpha|\mathcal{U}(t)|\varphi_\beta\rangle = \langle\varphi_\alpha|\varphi_\beta(t)\rangle\,. \tag{18}$$

8. Step 4: From (16) and (17) we find

$$\langle o|o(T)\rangle = \mathcal{U}_{1,1}(T)\,\langle e|e(T)\rangle = \langle\varphi_1|\varphi_1(T)\rangle\,\langle e|e(T)\rangle\,, \tag{19}$$

and therefore

$$e^{i\alpha_{\rm rel}} = \langle\varphi_1|\varphi_1(T)\rangle \tag{20}$$

That is, the relative phase is determined by the time evolution of the fermionic zero mode φ_1.

9. Step 5: The fermionic zero mode is a linear combination of two Majorana zero modes. To follow the time evolution of the fermionic one, it is insightful to use this Majorana decomposition. Along this line, an important auxiliary statement is the following. If our initial state for the time-dependent BdG equation is a Majorana zero mode, i.e., $\langle\sigma_xK\chi|\chi\rangle = 1$, then this property holds for the complete time evolution,

$$\langle\sigma_xK\chi(t)|\chi(t)\rangle = \langle\sigma_xK\mathcal{U}\chi|\mathcal{U}\chi\rangle = \langle\mathcal{U}\sigma_xK\chi|\mathcal{U}\chi\rangle = \langle\sigma_xK\chi|\chi\rangle = 1. \tag{21}$$

Note that although the Hamiltonian does not commute with the particle-hole symmetry operator, the propagator does, which we utilized in the second equality. This commutator property is proven here:

$$\sigma_xKe^{-\frac{i}{\hbar}\mathcal{H}(t)\delta t} \approx \sigma_xK\left[1 - \frac{i}{\hbar}\mathcal{H}(t)\delta t\right] = \left[1 + \frac{i}{\hbar}(-\mathcal{H}(t))\delta t\right]\sigma_xK \approx e^{-\frac{i}{\hbar}\mathcal{H}(t)\delta t}\sigma_xK. \tag{22}$$

10. Step 6: Now, we know that the two ends of the wire were exchanged adiabatically, therefore the time evolution of the Majorana zero modes must follow the Majorana zero modes of the instantaneous BdG matrix. From this it follows that there are 4 possible final configurations for the Majorana zero modes:

$$\chi_L(T) = \chi_R \text{ and } \chi_R(T) = \chi_L, \tag{23}$$
$$\chi_L(T) = \chi_R \text{ and } \chi_R(T) = -\chi_L, \tag{24}$$
$$\chi_L(T) = -\chi_R \text{ and } \chi_R(T) = \chi_L, \tag{25}$$
$$\chi_L(T) = -\chi_R \text{ and } \chi_R(T) = -\chi_L. \tag{26}$$

11. Step 7: Options (23) and (26) are excluded, since they would imply that the ground state has changed upon braiding, which is impossible. To make this explicit: e.g., we know that

$$\langle o(T)|d_1^\dagger d_1|o(T)\rangle = \langle o|d_1^\dagger d_1|o\rangle = 1, \tag{27}$$

but option (23) would imply

$$\langle o(T)|d_1^\dagger d_1|o(T)\rangle = \langle o|d_{H1}^\dagger(T) d_{H1}(T)|o\rangle = \langle o|d_1 d_1^\dagger|o\rangle = 0, \tag{28}$$

which is a contradiction.

12. Step 8: Consider, e.g., option (25). This implies

$$e^{i\alpha_{\rm rel}} = \langle\varphi_1|\varphi_1(T)\rangle = \frac{1}{2}\left(\langle\chi_L| - i\langle\chi_R|\right)\left(|\chi_L(T)\rangle + i|\chi_R(T)\rangle\right) = \frac{1}{2}\left(\langle\chi_L| - i\langle\chi_R|\right)\left(-|\chi_R\rangle + i|\chi_L\rangle\right) = i. \tag{29}$$

In the last step, we approximate the Majorana overlaps with as zero. Option (24) would imply $e^{i\alpha_{\rm rel}} = -i$.

13. To summarize: this proof does not rely on the assumption of homogeneity of the wire; disorder is allowed. The braiding results in an S gate if (i) braiding is slow enough (ii) system size is large enough so that the separation of Majorana zero modes is large and therefore the minigap is much suppressed, (iii) braiding should be fast enough, that is, faster than the time scale $\hbar/E_{\rm gap}$ defined by the minigap.

14. The BdG propagator can be utilized in a similar fashion to show that the B_{23} braiding provides an x rotation for the Majorana qubit, as stated above.